
An Optimization-based Approach To Node Role Discovery in Networks: Approximating Equitable Partitions

Michael Scholkemper

Department of Computer Science
RWTH Aachen University
scholkemper@cs.rwth-aachen.de

Michael T. Schaub

Department of Computer Science
RWTH Aachen University
schaub@cs.rwth-aachen.de

Abstract

Similar to community detection, partitioning the nodes of a network according to their structural roles aims to identify fundamental building blocks of a network. The found partitions can be used, e.g., to simplify descriptions of the network connectivity, to derive reduced order models for dynamical processes unfolding on processes, or as ingredients for various graph mining tasks. In this work, we offer a fresh look on the problem of role extraction and its differences to community detection and present a definition of node roles related to graph-isomorphism tests, the Weisfeiler-Leman algorithm and equitable partitions. We study two associated optimization problems (cost functions) grounded in ideas from graph isomorphism testing, and present theoretical guarantees associated to the solutions of these problems. Finally, we validate our approach via a novel “role-infused partition benchmark”, a network model from which we can sample networks in which nodes are endowed with different roles in a stochastic way.

1 Introduction

Networks are a powerful abstraction for a range of complex systems [31, 41]. To comprehend such networks we often seek patterns in their connections, e.g., core-periphery structures or densely knit communities. A complementary notion to community structure is that of a *role* partition of the nodes. The concept of node roles, or node equivalences, originates in social network analysis [22] and node roles are often related to symmetries or connectivity features that can be used to simplify complex networks. Contrary to communities, even nodes that are far apart or are part of different connected components of a network can have the same role [37].

Traditional approaches to define node roles, put forward in the context of social network analysis [7] consider *exact node equivalences*, based on structural symmetries within the graph structure. The earliest notion is that of *structural equivalence* [24], which assigns the same role to nodes if they are adjacent to the same nodes. Another definition is that of *automorphic equivalence* [13], which states that nodes are equivalent if they belong to the same automorphism orbits. Closely related is the idea of *regular equivalent* nodes [44], defined recursively as nodes that are adjacent to equivalent nodes.

However, large real-world networks often manifest in such a way that these definitions result in a vast number of different roles. What’s more, the above definitions do not define a similarity metric between nodes and it is thus not obvious how to compare two nodes that are deemed *not equivalent*. For example, the above definitions all have in common that nodes with different degrees also have different roles. With the aim of reducing a network’s complexity, this is detrimental.

To resolve this problem in a principled way and provide an effective partitioning of large graphs into nodes with similar roles, we present a quantitative definition of node roles in this paper. Our definition of roles is based on so-called *equitable partitions* (EPs), which are strongly related to

This research has been supported by the DFG RTG 2236 “UnRAVeL” – Uncertainty and Randomness in Algorithms, Verification and Logic.” and the Ministry of Culture and Science of North Rhine-Westphalia (NRW Rückkehrprogramm).

the notion of regular equivalence [44]. Crucially, this not only allows us to define an equivalence, but we can also quantify the deviation from an exact equivalence numerically. Further, the notion of EPs generalizes orbit partitions induced by automorphic equivalence classes in a principled way and thus remain tightly coupled to graph symmetries. Knowledge of EPs in a particular graph can, e.g., facilitate the computation of network statistics such as centrality measures [38]. As they are associated with certain spectral signatures, EPs are also relevant for the study of dynamical processes on networks such as cluster synchronization [32, 39], consensus dynamics [47], and network control problems [26]. They have even been shown to effectively imply an upper bound on the expressivity of Graph Neural Networks [28, 46].

Related Literature The survey by Rossi and Ahmed [35] puts forward an application-based approach to node role extraction that evaluates the node roles by how well they can be utilized in a downstream machine learning task. However, this perspective is task-specific and more applicable to node embeddings based on roles rather than the actual extraction of roles.

Apart from the already mentioned *exact* node equivalences originating from social network analysis, there exist numerous works on role extraction, which focus on finding nodes with *similar* roles, by associating each node with a feature vector that is independent of the precise location of the nodes in the graph. These feature vectors can then be clustered to assign nodes to roles. A recent overview article [37] puts forward three categories: First, graphlet-based approaches [33, 36, 23] use the number of graph homomorphisms of small structures to create node embeddings. This retrieves extensive, highly local information such as the number of triangles a node is part of. Second, walk-based approaches [2, 10] embed nodes based on certain statistics of random walks starting at each node. Finally, matrix-factorization-based approaches [16, 18] find a rank- r approximation of a node feature matrix ($F \approx MG$). Then, the left side multiplicand $M \in \mathbb{R}^{|V| \times r}$ of this factorization is used as a soft assignment of the nodes to r clusters.

Jin et al. [19] provide a comparison of many such node embedding techniques in terms of their ability to capture exact node roles such as structural, automorphic, and regular node equivalence. Detailed overviews of (exact) role extraction and its links to related topics such as block modeling are also given in [8, 9].

Contribution Our main contributions are as follows:

- We provide a principled stochastic notion of node roles, grounded in equitable partitions, which enables us to rigorously define node roles in complex networks.
- We provide a family of cost functions to assess the quality of a putative role partitioning. Specifically, using a depth parameter d we can control how much of a node’s neighborhood is taken into account when assigning roles.
- We present algorithms to minimize the corresponding optimization problems and derive associated theoretical guarantees.
- We develop a generative graph model that can be used to systematically test the recovery of roles in numerical experiments, and use this novel benchmark model to test our algorithms and compare them to well-known role detection algorithms from the literature.

2 Notation and Preliminaries

Graphs. A simple graph $G = (V, E)$ consists of a node set V and an edge set $E = \{uv \mid u, v \in V\}$. The neighborhood $N(v) = \{x \mid vx \in E\}$ of a node v is the set of all nodes connected to v . We allow self-loops $vv \in E$ and positive edge weights $w : E \rightarrow \mathbb{R}_+$.

Matrices. For a matrix M , $M_{i,j}$ is the component in the i -th row and j -th column. We use $M_{i,-}$ to denote the i -th row vector of M and $M_{-,j}$ to denote the j -th column vector. \mathbb{I}_n is the identity matrix and $\mathbb{1}_n$ the all-ones vector, both of size n respectively. Given a graph $G = (V, E)$, we identify the node set V with $\{1, \dots, n\}$. An *adjacency matrix* of a given graph is a matrix A with entries $A_{u,v} = 0$ if $uv \notin E$ and $A_{u,v} = w(uv)$ otherwise, where we set $w(uv) = 1$ for unweighted graphs for all $uv \in E$. $\rho(A)$ denotes the largest eigenvalue of the matrix A .

Partitions. A node partition $C = (C_1, C_2, \dots, C_k)$ is a division of the node set $V = C_1 \dot{\cup} C_2 \dot{\cup} \dots \dot{\cup} C_k$ into k disjoint subsets, such that each node is part of exactly one *class* C_i . For a node $v \in V$, we

write $C(v)$ to denote the class C_i where $v \in C_i$. We say a partition C' is coarser than C ($C' \supseteq C$) if $C'(v) \neq C'(u) \implies C(v) \neq C(u)$. For a partition C , there exists a partition indicator matrix $H \in \{0, 1\}^{|V| \times k}$ with $H_{i,j} = 1 \iff i \in C_j$.

2.1 Equitable Partitions.

An equitable partition (EP) is a partition $C = (C_1, C_2, \dots, C_k)$ such that $v, u \in C_i$ implies that

$$\sum_{x \in N(v)} [C(x) = C_j] = \sum_{x \in N(u)} [C(x) = C_j] \quad (1)$$

for all $1 \leq j \leq k$, where the Iverson bracket $[C(x) = C_j]$ is 1 if $C(x) = C_j$ and 0 otherwise. The coarsest EP (cEP) is the equitable partition with the minimum number of classes k . A standard algorithm to compute the cEP is the so-called Weisfeiler-Leman (WL) algorithm [43], which iteratively assigns a color $c(v) \in \mathbb{N}$ to each node $v \in V$ starting from a constant initial coloring. In each iteration, an update of the following form is computed:

$$c^{t+1}(v) = \text{hash}(c^t(v), \{\{c^t(x) | x \in N(v)\}\}) \quad (2)$$

where hash is an injective hash function, and $\{\{\cdot\}\}$ denotes a multiset (in which elements can appear more than once). In each iteration, the algorithm splits classes that do not conform with eq. (1). At some point T , the partition induced by the coloring no longer changes and the algorithm terminates returning the cEP as $\{(c^T)^{-1}(c^T(v)) | v \in V\}$. While simple, the algorithm is a powerful tool and is used as a subroutine in graph isomorphism testing algorithms [3, 27].

The above definition is useful algorithmically, but only allows to distinguish between exactly equivalent vs. non-equivalent nodes. To obtain a meaningful quantitative metric to gauge the quality of a partition, the following equivalent algebraic characterization of an EP will be instrumental: Given a graph G with adjacency matrix A and a partition indicator matrix H_{cEP} of the cEP, it holds that:

$$AH_{\text{cEP}} = H_{\text{cEP}}(H_{\text{cEP}}^\top H_{\text{cEP}})^{-1} H_{\text{cEP}}^\top A H_{\text{cEP}} =: H_{\text{cEP}} A^\pi. \quad (3)$$

The matrix $AH_{\text{cEP}} \in \mathbb{R}^{n \times k}$ counts in each row (for each node) the number of neighboring nodes within each class (C_i for $i = 1, \dots, k$), which has to be equal to $H_{\text{cEP}} A^\pi$ — a matrix in which each row (node) is assigned one of the k rows of the $k \times k$ matrix A^π . Thus, from any node v within in the same class C_i , the sum of edges from v to neighboring nodes of a given class C_k is equal to some fixed number — this is precisely the statement of Equation (1). The matrix A^π containing the connectivity statistics between the different classes is the adjacency matrix of the *quotient graph*, which has the following interesting properties. In particular, the adjacency matrix of the original graph inherits all eigenvalues from the quotient graph, as can be seen by direct computation. Specifically, let (λ, ν) be an eigenpair of A^π , then $AH_{\text{cEP}}\nu = H_{\text{cEP}}A^\pi\nu = \lambda H_{\text{cEP}}\nu$.

This makes EPs interesting from a dynamical point of view: the dominant (if unique) eigenvector is shared between the graph and the quotient graph. Hence, centrality measures such as Eigenvector Centrality or PageRank are predetermined if one knows the EP and the quotient graph [38]. For similar reasons, the cEP also provides insights into the long-term behavior of other (non)-linear dynamical processes such as cluster synchronization [39], consensus dynamics [47], or message passing graph neural networks. Recently, there has been some study on relaxing the notion of “*exactly*” equitable partitions. One approach is to compare the equivalence classes generated by eq. (2) by computing the edit distance of the trees (so called unravellings) that are encoded by these classes implicitly [17]. Another way is to relax the hash function (eq. (2)) to not be injective. This way, “buckets” of coarser equivalence classes are created [6]. Finally, using a less algorithmic perspective, one can define the problem of approximating EP by specifying a tolerance ϵ of allowed deviation from eq. (1) and consequently asking for the minimum number of clusters that still satisfy this constraint [20]. In this paper, we adopt the opposite approach and instead specify a number of clusters k and then ask for the partition minimizing a cost function (section 4) i.e. the *most equitable* partition with k classes. We want to stress that while similar, none of these relaxations coincide with our proposed approach.

2.2 The Stochastic Block Model

The Stochastic Block Model (SBM) [1] is a generative network model which assumes that the node set is partitioned into blocks. The probability of an edge between a node i and a node j is then only

dependent on the blocks $B(i)$ and $B(j)$. Given the block labels the expected adjacency matrix of a network sampled from the SBM fulfills:

$$\mathbb{E}[A] = H_B \Omega H_B^\top \quad (4)$$

where H_B is the indicator matrix of the blocks and $\Omega_{B(i),B(j)} = \Pr((i, j) \in E(G))$ is the probability with which an edge between the blocks $B(i)$ and $B(j)$ occurs.

For simplicity, we allow self-loops in the network. The SBM is used especially often in the context of community detection, in the form of the *planted partition model*.

In this restriction of the SBM, there is only an *inside* probability p and an *outside* probability q and $\Omega_{i,j} = p$ if $i = j$ and $\Omega_{i,j} = q$ if $i \neq j$. Usually, one also restricts $p > q$, to obtain a homophilic community structure i.e., nodes of the same class are more likely to connect. However, $p < q$ (heterophilic communities) are also sometimes considered.

3 Communities vs. Roles

In this section, we more rigorously define “communities” and “roles” and their difference. To this end, we first consider certain extreme cases and then see how we can relax them stochastically. Throughout the paper, we use the term communities synonymously with what is often referred to as *homophilic communities*, i.e., a community is a set of nodes that is more densely connected within the set than to the outside. In this sense, one may think of a *perfect* community partition into k communities if the network consists of k cliques. In contrast, we base our view of the term “role” on the cEP: If C is the cEP, then $C(v)$ is v 's *perfect* role. In this sense, the perfect role partition into k roles is present when the network has an exact EP with k classes. This can be seen in the appendix.

In real-world networks, such a perfect manifestation of communities and roles is rare. In fact, even if there was a real network with a perfect community (or role) structure, due to a noisy data collection process this structure would typically not be preserved. Hence, to make these concepts more useful in practice we need to relax them. For communities, the planted partition model relaxes this perfect notion of communities of disconnected cliques to a stochastic setting: The *expected adjacency matrix* exhibits perfect (weighted) cliques — even though each sampled adjacency matrix may not have such a clear structure. To obtain a principled stochastic notion of a node role, we argue that a *planted role model* should, by extension, have an exact cEP in expectation:

Definition 3.1. Two nodes $u, v \in V$ have the same *stochastic role* if they are in the same class in the cEP of $\mathbb{E}[A]$.

The above definition is very general. To obtain a practical generative model from which we can sample networks with a planted role structure, we concentrate on the following sufficient condition. We define a probability distribution over adjacency matrices such that for a given a role partition C , for $x, y \in C_i$ and classes C_j there exists a permutation $\sigma : C_j \rightarrow C_j$ such that $\Pr(A_{x,z} = 1) = \Pr(A_{y,\sigma(z)} = 1) \quad \forall z \in C_j$. That is: *two nodes have the same role if the stochastic generative process that links them to other nodes that have a certain role is the same up to symmetry*. Note that if we restrict σ to the identity, we recover the SBM. Therefore, we will consider the SBM as our stochastic generative process in the following.

RIP model In line with our above discussion we propose the *role-infused partition* (RIP) model, to create a well defined benchmark for role discovery, which allows to contrast role and community structure. The RIP model is fully described by the parameters $p \in \mathbb{R}, c, k, n \in \mathbb{N}, \Omega_{\text{role}} \in \mathbb{R}^{k \times k}$ as follows: We sample from an SBM with parameters Ω, H_B (see fig. 1) where

$$\Omega_{i,j} = \begin{cases} \Omega_{\text{role}_{i \bmod c, j \bmod c}} & \text{if } \lfloor \frac{i}{c} \rfloor = \lfloor \frac{j}{c} \rfloor \\ p & \text{otherwise} \end{cases} \quad (5)$$

where H_B corresponds to $c \cdot k$ blocks of size n . There are effectively c distinct communities, analogous to the planted partition model. The probability of nodes that are not in the same cluster to be adjacent is p . There are c distinct communities - analogous to the planted partition model. The probability of being adjacent for nodes that are not in the same community is p . In each community, there are the same k distinct roles with their respective probabilities to attach to one another as defined by Ω_{role} . Each role has n instances in each community.

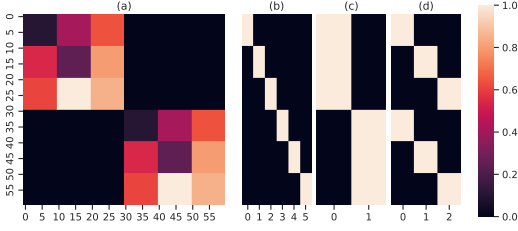


Figure 1: **Example of the RIP model**. It depicts (a) the expected adjacency matrix and the correct according to (b) SBM inference, (c) community detection, (d) role detection.

Input: Graph adjacency $A \in \{0, 1\}^{n \times n}$,
number of classes k

Output: Node assignment $H \in \{0, 1\}^{n \times k}$

- 1 $A = \text{normalize}(A)$
- 2 Initialize $H = \frac{1}{k} \mathbb{1}_n \mathbb{1}_k^T$
- 3 **for** *number of steps* **do**
- 4 $X = AH$
- 5 $H = \text{cluster}(X)$
- 6 **Return** H

Algorithm 1: Approximate Weisfeiler Lehman Algorithm.

Notice that the RIP model has both a planted community structure with c communities and a planted role structure, since $\mathbb{E}[A]$ has an *exact* cEP with k classes (definition 3.1). We stress that the central purpose of our model is to delineate the role recovery from community detection, i.e., community detection is *not* the endeavor of this paper. Rather, the planted communities within the RIP model are meant precisely as an alternative structure that can be found in the data and serve as a control mechanism to determine what structure an algorithm finds. To showcase this, consider Figure 1 which shows an example of the RIP model for $c = 2, k = 3, n = 10, p = 0.1$. It shows a graph that has 2 communities each of which can be subdivided into the same 3 roles. In standard SBM inference, one would like to obtain 6 blocks - each combination of community and role within being assigned its own block. In community detection with the objective to obtain 2 communities, the target clustering would be to merge the first 3 and the second 3 into one cluster respectively. However, the target clustering for this paper — aiming for 3 roles — is the one on the far right, combining from each community the nodes that have stochastically the same neighborhood structure.

4 Extracting Roles by Approximating the cEP

In this section, we define a family of cost functions (eq. 6, 7) that frame role extraction as an optimization problem. That is, we try to answer the question: *Given a desired number k of roles classes, what is the partition that is most like an EP?* As discussed above, searching for an *exact* equitable partition with a small number of classes is often not possible: It returns the singleton partition on almost all random graphs [4]. Already small asymmetries, or inaccuracies and noise in data collection can lead to a trivial cEP made up of singleton classes. As such, the cEP is not a robust nor a particularly useful choice for noisy or even just slightly asymmetric data. Our remedy to the problem is to search for coarser partitions that are closest to being equitable.

Considering the algebraic definition of cEP (eq. 1), intuitively one would like to minimize the difference between the left- and the right-hand side (throughout the paper, we use the ℓ_2 norm by default and the ℓ_1 norm where specified):

$$\Gamma_{\text{EP}}(A, H) = \|AH - HD^{-1}H^T AH\| \quad (6)$$

Here $D = \text{diag}(\mathbb{1}H)$ is the diagonal matrix with the sizes of the classes on its diagonal. We note that $HD^{-1}H^T = H(H^T H)^{-1}H^T = HH^\dagger$ is the projection onto the column space of H . However, eq. (6) disregards an interesting aspect that the *exact* cEP has. By its definition, the cEP is invariant under multiplication with A . That is,

$$A^t H_{\text{cEP}} = H_{\text{cEP}}(A^\pi)^t \quad \text{for all } t \in \mathbb{N}$$

This is especially interesting from a dynamical systems point of view since dynamics cannot leave the cEP subspace once they are inside it. Indeed, even complex dynamical systems such as Graph Neural Networks suffer from this restriction [46, 28]. To address this, we put forward the following family of cost functions.

$$\Gamma_{d\text{-EP}}(A, H) = \sum_{t=1}^d \frac{1}{\rho(A)^t} \Gamma_{\text{EP}}(A^t, H) \quad (7)$$

The factor of $\frac{1}{\rho(A)^t}$ is to rescale the impacts of each matrix power and not disproportionately enhance larger matrix powers. This family of cost functions measures how far the linear dynamical system

$t \mapsto A^t H$ diverges from a corresponding equitable dynamical system after d steps. Equivalently, it takes the d -hop neighborhood of each node into account when assigning roles. The larger d , the *deeper* it looks into the surroundings of a node. Note that all functions of this family have in common that if H_{cEP} indicates the exact cEP, then $\Gamma_{d\text{-EP}}(A, H_{\text{cEP}}) = 0$ for any choice of d .

In the following, we consider the two specific cost functions with extremal values of d for our theoretical results and our experiments: For $d = 1$, $\Gamma_{1\text{-EP}}$ is a measure of the variance of each node's adjacencies from the mean adjacencies in each class (and equivalent to eq. (6)). As such, it only measures the differences in the direct adjacencies and disregards the longer-range connections. We call this the *short-term* cost function. The other extreme we consider is $\Gamma_{\infty\text{-EP}}$, where $d \rightarrow \infty$. This function takes into account the position of a node within the whole graph. It takes into the long-range connectivity patterns around each node. We call this function the *long-term* cost.

In the following sections, we aim to optimize these objective functions to obtain a clustering of the nodes according to their roles. However, when optimizing this family of functions, in general, there exist examples where the optimal assignment is not isomorphism equivariant (See Appendix). As isomorphic nodes have *exactly* the same *global* neighborhood structure, arguably, they should be assigned the same role. To remedy this, we restrict ourselves to partitions compatible with the cEP when searching for the minimizer of these cost functions.

4.1 Optimizing the Long-term Cost Function

In this section, we consider optimizing the long-term objective eq. (7). This is closely intertwined with the dominant eigenvector of A , as the following theorem shows:

Theorem 4.1: *Let \mathcal{H} be the set of indicator matrices $H \in \{0, 1\}^{n \times k}$ s.t. $H \mathbb{1}_k = \mathbb{1}_n$. Let $A \in \mathbb{R}^{n \times n}$ be an adjacency matrix. Assume the dominant eigenvector to the eigenvalue $\rho(A)$ of A is unique. Using the ℓ_1 norm in eq. (6), the optimizer*

$$OPT = \arg \min_{H \in \mathcal{H}} \lim_{d \rightarrow \infty} \Gamma_{d\text{-EP}}(A, H)$$

can be computed in $\mathcal{O}(a + nk + n \log(n))$, where a is the time needed to compute the dominant eigenvector of A .

The proof of the theorem directly yields a simple algorithm that efficiently computes the optimal assignment for the long-term cost function. Simply compute the dominant eigenvector v and then cluster it using 1-dimensional k -means. We call this *EV-based clustering*.

4.2 Optimizing the Short-term Cost Function

In contrast to the previous section, the short-term cost function is more challenging. In fact,

Theorem 4.2: *Optimizing the short-term cost is NP-hard.*

In this section, we thus look into optimizing the short-term cost function by recovering the stochastic roles in the RIP model. Given s samples $A^{(s)}$ of the same RIP model, asymptotically, the sample mean $\frac{1}{s} \sum_{i=1}^s A^{(i)} \rightarrow \mathbb{E}[A]$ converges to the expectation as $s \rightarrow \infty$. Thus, recovering the ground truth partition is consistent with minimizing the short-term cost in expectation.

To extract the stochastic roles, we consider an approach similar to the WL algorithm which computes the exact cEP. We call this the approximate WL algorithm (Algorithm 1). A variant of this without the clustering step was proposed in [21]. Starting with one class encompassing all nodes, the algorithm iteratively computes an embedding vector $x = (x_1, \dots, x_k)$ for each node $v \in V$ according to the adjacencies of the classes:

$$x_i = \sum_{u \in N(v)} [C^{(t)}(u) = C_i^{(t)}]$$

The produced embeddings are then clustered to obtain the partition into k classes H of the next iteration. The clustering routine can be chosen freely. This is the big difference to the WL algorithm, which computes the number of classes on-the-fly — without an upper bound to the number of classes. The main theoretical result of this section uses average linkage for clustering:

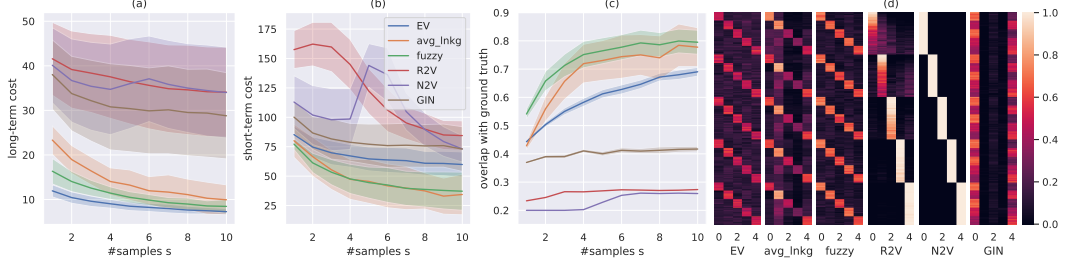


Figure 2: **Role recovery on graphs sampled from the RIP model .** (a-c) On the x-axis, we vary the number of samples s that are averaged to obtain the input A . The graphs used are randomly sampled from the planted partition model. On the y-axis, we report the long-term cost c_{20-EP} (a), the short-term cost (b) and the overlap of the coverings with the ground-truth (c) over 100 runs along with their standard deviation. In (d), the average role assignment (rows reordered to maximize overlap) is shown for the number of samples $s = 1$.

Theorem 4.3: *Let A be sampled from the RIP model with parameters $p \in \mathbb{R}, c \in \mathbb{N}, 3 \leq k \in \mathbb{N}, n \in \mathbb{N}, \Omega_{role} \in \mathbb{R}^{k \times k}$. Let $H_{role}^{(0)}, \dots, H_{role}^{(T')}$ be the indicator matrices of each iteration when performing the exact WL algorithm on $\mathbb{E}[A]$. Let $\delta = \min_{0 \leq t' \leq T'} \min_{i \neq j} \|(\Omega H_{role}^{(t')})_{i,-} - (\Omega H_{role}^{(t')})_{j,-}\|$. Using average linkage in algorithm 1 in the clustering step and assuming the former correctly infers k , if*

$$n > -\frac{9\mathcal{W}_{-1}((q-1)\delta^2/9k^2)}{2\delta^2} \quad (8)$$

where \mathcal{W} is the Lambert W function, then with probability at least q : Algorithm 1 finds the correct role assignment using average linkage for clustering.

The proof hinges on the fact that the number of links from each node to the nodes of any class concentrates around the expectation. Given a sufficient concentration, the correct partitioning can then be determined by the clustering step. Notice, that even though we allow for the SBM to have more blocks than there are roles, the number of roles (and the number of nodes therein) is the delimiting factor here - not the overall number of nodes. Notice also that theorem 4.3 refers to *exactly* recovering the partition from only *one* sample. Typically, concentration results refer to a concentration of multiple samples from the same model. Such a result can be derived as a direct consequence of Theorem 4.3 and can be found in the appendix. The bound given in the theorem is somewhat crude in the sense that it scales very poorly as δ decreases. This is to be expected as the theorem claims exact recovery for all nodes with high probability.

Fractional Assignments In a regime, where the conditions of Theorem 4.3 do not hold, it may be beneficial to relax the problem. A hard assignment in intermediate iterations, while possible, has shown to be empirically unstable (see experiments). Wrongly assigned nodes heavily impact the next iteration of the algorithm. As a remedy, a soft assignment - while not entirely different - has proven more robust. We remain concerned with finding the minimizer H of eq. (6) However, we no longer constrain $H_{i,j} \in \{0, 1\}$, but relax this to $0 \leq H_{i,j} \leq 1$. H must still be row-stochastic - i.e. $H\mathbf{1} = \mathbf{1}$. That is, a node may now be *fractionally* assigned to multiple classes designating how strongly it belongs to each class. This remedies the above problems, as algorithms such as Fuzzy c -means or Bayesian Gaussian Mixture Models are able to infer the number of clusters at runtime and must also not make a hard choice about which cluster a node belongs to. This also allows for Gradient Descent approaches like e.g. GNNs. We investigate these thoughts empirically in the experiments section.

5 Numerical Experiments

For the following experiments, we use two variants of the approximate WL algorithm (1), one where the clustering is done using average linkage and one where fuzzy c -means is used. We benchmark the EV-based clustering (4.1) and the 2 variants of the approximate WL algorithm as well as node classes obtained from the role2vec [2] and the node2vec [15] node embeddings (called $R2V$ and $N2V$ in the figures). We retrieve an assignment from the two baseline benchmark embeddings by k -means. Both node embedding techniques use autoencoders with skip-gram to compress information obtained by

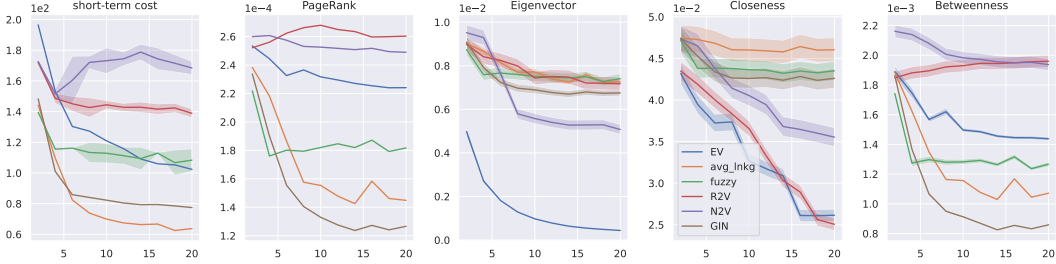


Figure 3: **Recovery of centralities on a real-world network.** On the x-axis, the number of classes $2 \leq k \leq 20$ that the algorithms are tasked to find is shown. On the y-axis, the mean short-term cost c_{EP} , the average deviation from the cluster mean is then shown from left to right for PageRank, Eigenvector centrality, Closeness and Betweenness over 10 trials on the protein dataset.

random walks. While node2vec is a somewhat universal node embedding technique also taking into account the community structure of a network, role2vec is focussed on embedding a node due to its role. Both embeddings are state-of-the-art node embedding techniques used for many downstream tasks. Further, we compare the above algorithms to the GIN [46] which is trained to minimize the short-term cost individually on each graph. The GIN uses features of size 32 that are uniformly initialized and is trained for 1000 epochs. To enable a fair comparison, we convert the fractional assignments into hard assignments by taking the class with the highest probability for each node. Experimental data and code will be made available here.

Experiment 1: Planted Role Recovery. For this experiment, we sampled adjacency matrices $A^{(i)}$ from the RIP model as described in section 3 with $c = k = 5, n = 10, p = 0.05, \Omega_{\text{role}} \in \mathbb{R}^{k \times k}$. Each component of Ω_{role} is sampled uniformly at random i.i.d from the interval $[0, 1]$. We then sample s samples from this RIP model and perform the algorithms on the sample mean. The mean and standard deviation of long-term and short-term costs and the mean recovery accuracy of the ground truth and its variance are reported in Figure 2 over 100 trials for each value of s . The overlap score of the assignment C with the ground truth role assignment C^{gt} is computed as:

$$\text{overlap}(C, C^{\text{gt}}) = \max_{\sigma \in \text{permutations}(\{1, \dots, k\})} \sum_{i=1}^k \frac{|C_{\sigma(i)} \cap C_i^{\text{gt}}|}{|C_i|}$$

Figure 2 (d) shows the mean role assignments output by each algorithm. Since the columns of the output indicator matrix H of the algorithms are not ordered in any specific way, we use the maximizing permutation σ to align the columns before computing the average.

Discussion. In Figure 2 (a), one can clearly see that the EV-based clustering outperforms all other algorithms measured by long-term cost, validating Theorem 4.1. While both approximate WL algorithms perform similarly in the cost function, the fuzzy variant has a slight edge in recovery accuracy. We can see that the tendencies for the short-term cost and the accuracy are directly adverse. The Approximate WL algorithms have the lowest cost and also the highest accuracy in recovery. The trend continues until both X2vec algorithms are similarly bad in both measures. The GIN performs better than the X2vec algorithms both in terms of cost and accuracy. However, it mainly finds 2 clusters. This may be because of the (close to) uniform degree distribution in these graphs.

On the contrary, the X2vec algorithms detect the communities instead of the roles. This is surprising for role2vec since it aims to detect roles.

Experiment 2: Inferring the Number of Roles and Centrality. A prominent problem in practice that has been scarcely addressed in this paper so far is that the number of roles may not be known. Some algorithms — like fuzzy c -means or GIN — can infer the number of clusters while performing the clustering. In this experiment, we consider the *protein* dataset [5] and run the suite of algorithms for varying $2 \leq k \leq 20$. The mean short-term cost of the assignments and its standard deviation is reported in Figure 3. Additionally for the PageRank, Eigenvector, Closeness and Betweenness Centrality, the l_1 deviations of each node from the mean cluster value are reported.

Discussion. In Figure 3, all algorithms show a similar trend. The cost decreases as the number of clusters increases. The elbow method yields $k = 4, 6$ depending on the algorithm. The GIN

Table 1: **Few shot graph embedding performance** Mean accuracy in % over 10 runs of the EV embedding, Graph2Vec and the GIN. For each run we randomly sample 10 data points for training and evaluate with the rest. As a comparison, the GIN+ is trained on 90% of the data points.

	EV	G2Vec	GIN	GIN+
AIDS	95.0 \pm 5.2	79.9 \pm 4.4	80.0 \pm 14.1	97.8 \pm 1.4
ENZYMES	21.3 \pm 1.7	20.3 \pm 1.5	21.0 \pm 1.7	60.3 \pm 0.7
PROTEINS	66.5 \pm 6.4	60.3 \pm 3.5	59.6 \pm 7.6	75.4 \pm 1.3
NCII	58.5 \pm 4.0	53.9 \pm 1.5	50.0 \pm 1.4	82.0 \pm 0.3
MUTAG	81.5 \pm 7.7	66.9 \pm 5.6	77.5 \pm 11.1	94.3 \pm 0.5

performs much better than in the previous experiment. This may be due to the fact that there are some high-degree nodes in the dataset, that are easy to classify correctly. The converse is true for the fuzzy variant of approximate WL that implicitly assumes that all clusters should have about the same size. The EV algorithm clusters the nodes well in terms of Eigenvector centrality which is to be expected. However, the clustering produced by the GIN also clusters the network well in terms of PageRank and Betweenness centrality.

Experiment 3: Graph Embedding. In this section, we diverge a little from the optimization-based perspective of the paper up to this point and showcase the effectiveness of the information content of the extracted roles in a few-shot learning downstream task. This links our approach to the application-based role evaluation approach of [35]. We employ an embedding based on the minimizer of the long-term cost function (eq. (7), Algorithm 4.1). The embedding is defined as follows: Let A be the adjacency matrix of the graph that is to be embedded. Let $C = \{C_1, \dots, C_k\}$ be the optimal clustering found by the 1d-kmeans algorithm on the dominant eigenvector v of A . The embedding is then made up of the cluster sizes together with the cluster centers.

$$\text{EV}_{\text{emb}} = (|C_1|, \dots, |C_k|, \frac{1}{|C_1|} \sum_{i \in C_1} v_i, \dots, \frac{1}{|C_k|} \sum_{i \in C_k} v_i)$$

The value for k was found by a grid search over $k \in \{2, \dots, 20\}$. We benchmark this against the commonly used graph embedding Graph2Vec [30] and the GIN. We use graph classification tasks from the field of bioinformatics ranging from 188 graphs with an average of 18 nodes to 4110 graphs with an average of 30 nodes. The datasets are taken from [29] and were first used (in order of table 1) in [34, 40, 12, 42, 11]. In each task, we use only 10 data points to train a 2-layer MLP on the embeddings and a 4-layer GIN. Each hidden MLP and GIN layer has 100 nodes. The Graph2Vec embedding is set to size 16, whereas the GIN receives as embedding the attributes of the nodes of the respective task. The GIN is thus *informed*. We also report the accuracy of a GIN that is trained on 90% of the respective data sets. The results over 10 independent runs are reported in table 1.

Discussion. Experiment 3 has the EV embedding as the overall winner of few-shot algorithms. Our claim here is not that the EV embedding is a particularly powerful few-shot learning approach, but that the embedding carries a lot of structural information. Not only that but it is robust in the sense that few instances are enough to train a formidable classifier. However, it pales in comparison with the “fully trained” GIN, which is better on every dataset.

6 Conclusion

We proposed an optimization-based framework for role extraction aiming to optimize two cost functions. Each measures how well a certain characteristic of the cEP is upheld. We proposed an algorithm for finding the optimal clustering for the long-term cost function and related the optimization of the other cost function to the retrieval of stochastic roles from the RIP model .

Limitations The proposed cost functions are sensitive to the degree of the nodes. In scale-free networks, for example, it can happen that few extremely high-degree nodes are put into singleton clusters and the many remaining low-degree nodes are placed into one large cluster. The issue is somewhat reminiscent of choosing a minimal min-cut when performing community detection, which may result in a single node being cut off from the main graph. A remedy akin to using a normalized cut may thus be a helpful extension to our optimization-based approach. Future work may thus consider correcting for the degree, and a further strengthening of our theoretic results.

References

- [1] E. Abbe. Community detection and stochastic block models: recent developments. *The Journal of Machine Learning Research*, 18(1):6446–6531, 2017.
- [2] N. K. Ahmed, R. A. Rossi, J. B. Lee, T. L. Willke, R. Zhou, X. Kong, and H. Eldardiry. role2vec: Role-based network embeddings. *Proc. DLG KDD*, pages 1–7, 2019.
- [3] L. Babai. Graph isomorphism in quasipolynomial time. In *Proceedings of the forty-eighth annual ACM symposium on Theory of Computing*, pages 684–697, 2016.
- [4] L. Babai and L. Kucera. Canonical labelling of graphs in linear average time. In *20th Annual Symposium on Foundations of Computer Science*, pages 39–46. IEEE, 1979.
- [5] A. Barabási. Networkscience book datasets. URL <http://networksciencebook.com/resources/data.html>. Accessed: 2022-10-01.
- [6] F. Bause and N. M. Kriege. Gradual weisfeiler-leman: Slow and steady wins the race. In *Learning on Graphs Conference*, pages 20–1. PMLR, 2022.
- [7] U. Brandes. *Network analysis: methodological foundations*, volume 3418. Springer Science & Business Media, 2005.
- [8] A. Browet. *Algorithms for community and role detection in networks*. PhD thesis, Catholic University of Louvain, Belgium, 2014.
- [9] T. P. Cason. *Role extraction in networks*. PhD thesis, Catholic University of Louvain, Belgium, 2012.
- [10] K. Cooper and M. Barahona. Role-based similarity in directed networks. *arXiv preprint arXiv:1012.2726*, 2010.
- [11] A. K. Debnath, R. L. Lopez de Compadre, G. Debnath, A. J. Shusterman, and C. Hansch. Structure-activity relationship of mutagenic aromatic and heteroaromatic nitro compounds. correlation with molecular orbital energies and hydrophobicity. *Journal of medicinal chemistry*, 34(2):786–797, 1991.
- [12] P. D. Dobson and A. J. Doig. Distinguishing enzyme structures from non-enzymes without alignments. *Journal of molecular biology*, 330(4):771–783, 2003.
- [13] M. G. Everett and S. P. Borgatti. Regular equivalence: General theory. *Journal of mathematical sociology*, 19(1):29–52, 1994.
- [14] A. Grønlund, K. G. Larsen, A. Mathiasen, J. S. Nielsen, S. Schneider, and M. Song. Fast exact k-means, k-medians and bregman divergence clustering in 1d. *arXiv preprint arXiv:1701.07204*, 2017.
- [15] A. Grover and J. Leskovec. node2vec: Scalable feature learning for networks. In *Proceedings of the 22nd ACM SIGKDD international conference on Knowledge discovery and data mining*, pages 855–864, 2016.
- [16] K. Henderson, B. Gallagher, T. Eliassi-Rad, H. Tong, L. Akoglu, D. Koutra, L. Li, S. Basu, and C. Faloutsos. Rolx: Role extraction and mining in large networks. Technical report, Lawrence Livermore National Lab, Livermore, CA (United States), 2011.
- [17] T. Hendrik Schulz, T. Horváth, P. Welke, and S. Wrobel. A generalized weisfeiler-lehman graph kernel. *arXiv e-prints*, pages arXiv–2101, 2021.
- [18] D. Jin, M. Heimann, T. Safavi, M. Wang, W. Lee, L. Snider, and D. Koutra. Smart roles: Inferring professional roles in email networks. In *Proceedings of the 25th ACM SIGKDD International Conference on Knowledge Discovery & Data Mining*, pages 2923–2933, 2019.
- [19] J. Jin, M. Heimann, D. Jin, and D. Koutra. Towards understanding and evaluating structural node embeddings. *arXiv preprint arXiv:2101.05730*, 2021.

- [20] M. Kayali and D. Suci. Quasi-stable coloring for graph compression: Approximating max-flow, linear programs, and centrality. *arXiv preprint arXiv:2211.11912*, 2022.
- [21] K. Kersting, M. Mladenov, R. Garnett, and M. Grohe. Power iterated color refinement. In *Proceedings of the AAAI Conference on Artificial Intelligence*, volume 28, 2014.
- [22] D. Knoke and S. Yang. *Social network analysis*. Sage Publications, 2019.
- [23] X. Liu, Y.-Z. J. Chen, J. C. Lui, and K. Avrachenkov. Learning to count: A deep learning framework for graphlet count estimation. *Network Science*, page 30, 2020.
- [24] F. Lorrain and H. C. White. Structural equivalence of individuals in social networks. *The Journal of mathematical sociology*, 1(1):49–80, 1971.
- [25] M. Mahajan, P. Nimbhorkar, and K. Varadarajan. The planar k-means problem is np-hard. *Theoretical Computer Science*, 442:13–21, 2012.
- [26] S. Martini, M. Egerstedt, and A. Bicchi. Controllability analysis of multi-agent systems using relaxed equitable partitions. *International Journal of Systems, Control and Communications*, 2(1-3):100–121, 2010.
- [27] B. D. McKay and A. Piperno. Practical graph isomorphism, ii. *Journal of symbolic computation*, 60:94–112, 2014.
- [28] C. Morris, M. Ritzert, M. Fey, W. L. Hamilton, J. E. Lenssen, G. Rattan, and M. Grohe. Weisfeiler and leman go neural: Higher-order graph neural networks. In *Proceedings of the AAAI Conference on Artificial Intelligence*, volume 33, pages 4602–4609, 2019.
- [29] C. Morris, N. M. Kriege, F. Bause, K. Kersting, P. Mutzel, and M. Neumann. Tudataset: A collection of benchmark datasets for learning with graphs. In *ICML 2020 Workshop on Graph Representation Learning and Beyond (GRL+ 2020)*, 2020. URL www.graphlearning.io.
- [30] A. Narayanan, M. Chandramohan, R. Venkatesan, L. Chen, Y. Liu, and S. Jaiswal. graph2vec: Learning distributed representations of graphs. *arXiv preprint arXiv:1707.05005*, 2017.
- [31] M. Newman. *Networks*. Oxford University Press, 2018.
- [32] L. M. Pecora, F. Sorrentino, A. M. Hagerstrom, T. E. Murphy, and R. Roy. Cluster synchronization and isolated desynchronization in complex networks with symmetries. *Nature communications*, 5(1):1–8, 2014.
- [33] N. Pržulj. Biological network comparison using graphlet degree distribution. *Bioinformatics*, 23(2):e177–e183, 2007.
- [34] K. Riesen and H. Bunke. Iam graph database repository for graph based pattern recognition and machine learning. In *Joint IAPR International Workshops on Statistical Techniques in Pattern Recognition (SPR) and Structural and Syntactic Pattern Recognition (SSPR)*, pages 287–297. Springer, 2008.
- [35] R. A. Rossi and N. K. Ahmed. Role discovery in networks. *IEEE Transactions on Knowledge and Data Engineering*, 27(4):1112–1131, 2014.
- [36] R. A. Rossi, R. Zhou, and N. K. Ahmed. Estimation of graphlet counts in massive networks. *IEEE Transactions on Neural Networks and Learning Systems*, 30(1):44–57, 2018.
- [37] R. A. Rossi, D. Jin, S. Kim, N. K. Ahmed, D. Koutra, and J. B. Lee. On proximity and structural role-based embeddings in networks: Misconceptions, techniques, and applications. *ACM Transactions on Knowledge Discovery from Data (TKDD)*, 14(5):1–37, 2020.
- [38] R. J. Sánchez-García. Exploiting symmetry in network analysis. *Communications Physics*, 3(1):1–15, 2020.
- [39] M. T. Schaub, N. O’Clery, Y. N. Billeh, J.-C. Delvenne, R. Lambiotte, and M. Barahona. Graph partitions and cluster synchronization in networks of oscillators. *Chaos: An Interdisciplinary Journal of Nonlinear Science*, 26(9):094821, 2016.

- [40] I. Schomburg, A. Chang, C. Ebeling, M. Gremse, C. Heldt, G. Huhn, and D. Schomburg. Brenda, the enzyme database: updates and major new developments. *Nucleic acids research*, 32(suppl_1):D431–D433, 2004.
- [41] S. H. Strogatz. Exploring complex networks. *Nature*, 410(6825):268–276, 2001.
- [42] N. Wale, I. A. Watson, and G. Karypis. Comparison of descriptor spaces for chemical compound retrieval and classification. *Knowledge and Information Systems*, 14(3):347–375, 2008.
- [43] B. Weisfeiler and A. Leman. The reduction of a graph to canonical form and the algebra which appears therein. *NTI, Series*, 2(9):12–16, 1968.
- [44] D. R. White and K. P. Reitz. Graph and semigroup homomorphisms on networks of relations. *Social Networks*, 5(2):193–234, 1983.
- [45] X. Wu. Optimal quantization by matrix searching. *Journal of algorithms*, 12(4):663–673, 1991.
- [46] K. Xu, W. Hu, J. Leskovec, and S. Jegelka. How powerful are graph neural networks? *arXiv preprint arXiv:1810.00826*, 2018.
- [47] Y. Yuan, G.-B. Stan, L. Shi, M. Barahona, and J. Goncalves. Decentralised minimum-time consensus. *Automatica*, 49(5):1227–1235, 2013.

Supplementary Material

A Example of Communities vs. Roles

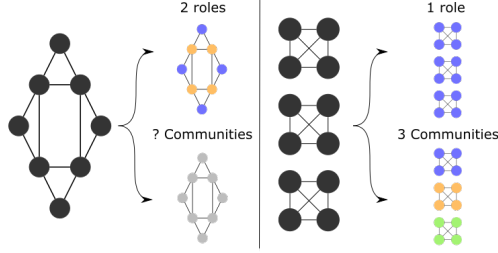


Figure 4: **Toy example** showing two networks and their role/community structure. The left has two *exact* roles but how many communities it has is not clear. The right has 3 *perfect* communities, but only a single role.

B Example of Isomorphic Nodes that receive a different role

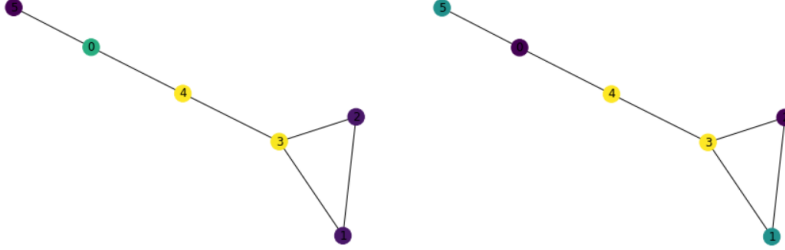


Figure 5: **Example graphs** showing undesirable properties of the optimizer of eq. (6). Nodes 1 and 2 are in the same cEP class; they are even isomorphic. However, the minimizer of eq. (6) puts them into different classes. The partition minimizing eq. (6) as given by the right yields a score of 0.707, whereas the best partition that respects the cEP yields 0.816.

C Proof of theorem 4.1

Theorem 4.1: *Let \mathcal{H} be the set of indicator matrices $H \in \{0, 1\}^{n \times k}$ s.t. $H\mathbb{1}_k = \mathbb{1}_n$. Let $A \in \mathbb{R}^{n \times n}$ be an adjacency matrix. Assume the dominant eigenvector to the eigenvalue $\rho(A)$ of A is unique. Using the ℓ_1 norm in eq. (6), the optimizer*

$$OPT = \arg \min_{H \in \mathcal{H}} \lim_{d \rightarrow \infty} \Gamma_{d-EP}(A, H)$$

can be computed in $\mathcal{O}(a + nk + n \log(n))$, where a is the time needed to compute the dominant eigenvector of A .

Proof. Consider the long-term cost function (eq. 6,7):

$$\begin{aligned} c_{d-EP}(A, H) &= \sum_t^d \frac{1}{\rho(A)^t} \|A^t H - H D^{-1} H^\top A^t H\| \\ &= \sum_t^d \|(\mathbb{I}_n - H D^{-1} H^\top) \frac{1}{\rho(A)^t} A^t H\| \\ &\stackrel{\lim_{d \rightarrow \infty}}{=} \|(\mathbb{I}_n - H D^{-1} H^\top) w v^\top H\| \end{aligned}$$

We arrive at a formulation akin to the k -means cost function. However, $w v^\top H$ is in general not independent of the clustering, as would be the case in the usual formulation of k -means. This can be

used advantageously by rewriting the above matrix equation element-wise:

$$\begin{aligned} &= \sum_i^n \sum_j^k |w_i(v^\top H_{-,j}) - \frac{1}{|C(w_i)|} \sum_{l \in C(w_i)} w_l(v^\top H_{-,j})| \\ &= \sum_i^n \sum_j^k |(w_i - \frac{1}{|C(w_i)|} \sum_{l \in C(w_i)} w_l)(v^\top H_{-,j})| \end{aligned}$$

It is possible to completely draw out the constant factor of $\sum_j v^\top H_{-,j} = \sum_i v_i$ since the row sums of H are 1 and the components $v_i \geq 0$ are non-negative.

$$\begin{aligned} &= \sum_i^n \sum_j^k (v^\top H_{-,j}) |(w_i - \frac{1}{|C(w_i)|} \sum_{l \in C(w_i)} w_l)| \\ &= \text{const} \sum_i^n |(w_i - \frac{1}{|C(w_i)|} \sum_{l \in C(w_i)} w_l)| \end{aligned}$$

We end up at a formulation equivalent to clustering w into k clusters using k -means. We can now notice that w is only 1-dimensional and as such the k -means objective can be optimized in $\mathcal{O}(n \log(n) + nk)$ [45, 14]. \square

D Proof of theorem 4.2

Theorem 4.2: *Optimizing the short-term cost is NP-hard.*

Proof. We reduce from the PLANAR-K-MEANS problem, which is shown to be NP-hard in [25]. In PLANAR-K-MEANS, we are given a set $\{(x_1, y_1), \dots, (x_n, y_n)\}$ of n points in the plane and a number k and a cost c . The problem is to find a partition of the points into k clusters such that the cost of the partition is at most c , where the cost of a partition is the sum of the squared distances of each point to the center of its cluster. We now formulate the decision variant of optimizing the short-term cost which we show is NP-hard.

Definition D.1 (K-AEP). Let $G = (V, E)$ be a graph, $k \in \mathbb{N}$ and $c \in \mathbb{R}$. K-AEP is then the problem of deciding whether there exists a partition of the nodes in V into k clusters such that the short-term cost $\Gamma_{1\text{-EP}}$ (eq. (7)) using the squared L2 norm is at most c .

Let $W(X, Y)$ be the sum of the weights of all edges between $X, Y \subseteq V$. Additionally, for a given partition indicator matrix H , let C_i be the set of nodes v s.t. $H_{v,i} = 1$. For the following proof, the equivalent definition of the short-term cost function (eq. 6) using the squared L2 norm is more convenient:

$$\Gamma_{\text{EP}}(A, H) = \sum_i \sum_j \sum_{v \in C_i} (W(\{v\}, C_j) - \frac{1}{|C_i|} W(C_i, C_j))^2$$

We now show that K-AEP is NP-hard by reduction from PLANAR-K-MEANS.

Construction. Given $\{(x_1, y_1), \dots, (x_n, y_n)\}$ of n points in the plane and a number k' and a cost c' construct the following graph: We shift the given points by $-\min_{i \in [n]} x_i$ in their x -coordinate and by $-\min_{i \in [n]} y_i$ in their y -coordinate. This makes them non-negative, but does not change the problem. Let $D = 1 + \sum_{i=1}^n x_i^2 + y_i^2$. Notice that D is an upper bound on the cost of the k -means partition. To start, let $V = \{a, b\}$. Add self-loops of weight $3D$ to a and of weight $6D$ to b . For each point (x_i, y_i) , add a node m_i to V and add edges $m_i a$ of weight x_i and $m_i b$ of weight y_i to E .

$G = (V, E), k = k' + 2, c = c'$ are now the inputs to K-AEP.

Correctness. We now prove that the PLANAR-K-MEANS instance has a solution if and only if K-AEP has a solution. Assume that PLANAR-K-MEANS has a solution $S' = (S'_1, \dots, S'_{k'})$ that has

cost $c^* \leq c'$. Then the solution we construct for K-AEP is $S = (S_1, \dots, S_{k'}, \{a\}, \{b\})$, where $m_i \in S_j \iff (x_i, y_i) \in S'_j$. The cost of this solution is:

$$c^+ = \sum_{i=1}^k \sum_{j=1}^k \sum_{v \in S_i} (W(\{v\}, S_j) - \frac{1}{|S_i|} W(S_i, S_j))^2$$

Since a and b are in singleton clusters, their outgoing edges do not differ from the cluster average and so incur no cost. The remaining edges either go from $V \setminus \{a, b\}$ to a or from $V \setminus \{a, b\}$ to b . So, the sum reduces to:

$$c^+ = \sum_i \sum_{v \in S_i} \left((w(v, a) - \frac{1}{|S_i|} W(S_i, \{a\}))^2 + (w(v, b) - \frac{1}{|S_i|} W(S_i, \{b\}))^2 \right)$$

Since $\mu_x(S_i) := \frac{1}{|S_i|} W(S_i, \{a\})$ is the average weight of the edges from S_i to a , and these edges have weight according to the x coordinate of the point they were constructed from, $\mu_x(S_i)$ is equal to the mean x coordinate within the cluster S'_i . This concludes the proof of this direction, as:

$$c^+ = \sum_{S'_i \in S'} \sum_{(x_l, y_l) \in S'_i} (x_l - \mu_x(S'_i))^2 + (y_l - \mu_y(S'_i))^2 = c^* \leq c'$$

For the other direction, assume we are given a solution $S = (S_1, \dots, S_{k+2})$ to K-AEP with cost $c^+ \leq c$. We distinguish two cases:

Case 1: $\exists i \in \mathbb{N}$ s.t. $S_i \supseteq \{a\}$ or $S_i \supseteq \{b\}$. Assume that $S_i \supseteq \{a\}$, if also $b \in S_i$ then the cost is at least the difference of the two self-loops:

$$\begin{aligned} c^+ &\geq \sum_{v \in S_i} \left(W(\{v\}, S_i) - \frac{1}{|S_i|} W(S_i, S_i) \right)^2 \\ &\geq \left(\frac{1}{2} \max_{u, v \in S_i} W(\{v\}, S_i) - W(\{u\}, S_i) \right)^2 \\ &\geq \left(\frac{1}{2} (w(b, b) - W(\{a\}, S_i)) \right)^2 \\ &\geq \left(\frac{1}{2} (6D - 4D) \right)^2 = D^2 \geq D \end{aligned}$$

If instead, some $m_j \in S_i$, then the cost is at least the difference of the self-loop to a and the edge from m_j to a :

$$\begin{aligned} c^+ &\geq \sum_{v \in S_i} \left(W(\{v\}, S_i) - \frac{1}{|S_i|} W(S_i, S_i) \right)^2 \\ &\geq \left(\frac{1}{2} (w(a, a) - W(\{m_j\}, S_i)) \right)^2 \\ &\geq \left(\frac{1}{2} (3D - D) \right)^2 = D^2 \geq D \end{aligned}$$

Thus $c^+ \geq D$ is so large that any clustering of the points has at most cost $c \geq D$ thus a solution to the PLANAR-K-MEANS instance exists. The case where $S_i \supseteq \{b\}$ is analogous.

Case 2: *Case 1 doesn't hold.* In this case, we have $S = (S_1, \dots, S_k, \{a\}, \{b\})$ which yields a clustering $S' = (S'_1, \dots, S'_k)$ for the PLANAR-K-MEANS, where $m_i \in S_j \iff (x_i, y_i) \in S'_j$. This instance has cost $c^+ = c^* \leq c$. \square

E Proof of theorem 4.3

Theorem 4.3: *Let A be sampled from the RIP model with parameters $p \in \mathbb{R}, c \in \mathbb{N}, 3 \leq k \in \mathbb{N}, n \in \mathbb{N}, \Omega_{role} \in \mathbb{R}^{k \times k}$. Let $H_{role}^{(0)}, \dots, H_{role}^{(T')}$ be the indicator matrices of each iteration*

when performing the exact WL algorithm on $\mathbb{E}[A]$. Let $\delta = \min_{0 \leq t' \leq T'} \min_{i \neq j} \|(\Omega H_{role}^{(t')})_{i,-} - (\Omega H_{role}^{(t')})_{j,-}\|$. Using average linkage in algorithm 1 in the clustering step and assuming the former correctly infers k , if

$$n > -\frac{9\mathcal{W}_{-1}((q-1)\delta^2/9k^2)}{2\delta^2} \quad (8)$$

where \mathcal{W} is the Lambert W function, then with probability at least q : Algorithm 1 finds the correct role assignment using average linkage for clustering.

Proof. Consider the adjacency matrix A_B of a simple binomial random graph of size n - i.e. a single block of the SBM. Let $\delta^* < \frac{\delta}{3}$. Using the Chernoff bound for binomial random variables, we have that the degree of a single node i is within the ball of size δ^* with probability:

$$\Pr(|(A_B \mathbb{1})_i - \mathbb{E}[(A_B \mathbb{1})_i]| \geq \delta^* \cdot n) \leq 2e^{-2n(\delta^*)^2}$$

The probability that all nodes fall in close proximity to the expectation, is then simply:

$$\Pr(\|A_B \mathbb{1} - \mathbb{E}[A_B \mathbb{1}]\|_\infty \geq \delta^* \cdot n) \leq (1 - 2e^{-2n(\delta^*)^2})^n$$

Finally, in the SBM setting, we have k^2 such blocks and the probability that none of the nodes are far away from the expectation in any of these blocks is:

$$\Pr\left(\left\|\frac{AHH_{role}^{(T)} - \mathbb{E}[AHH_{role}^{(T)}]}{n}\right\| \geq \delta^*\right) \leq (1 - 2e^{-2n(\delta^*)^2})^{nk^2}$$

We can upper bound this by its first-order Taylor approximation:

$$\begin{aligned} (1 - 2e^{-2n(\delta^*)^2})^{nk^2} &\leq p \leq 1 - 2nk^2e^{-2n(\delta^*)^2} \\ \Leftrightarrow \frac{(p-1)(\delta^*)^2}{k^2} &\leq -2n(\delta^*)^2e^{-2n(\delta^*)^2} \\ \Leftrightarrow \mathcal{W}_{-1}\left(\frac{(p-1)(\delta^*)^2}{k^2}\right) &\geq -2n(\delta^*)^2 \\ \Leftrightarrow -\frac{9\mathcal{W}_{-1}((p-1)\delta^2/9k^2)}{2\delta^2} &\leq n \end{aligned}$$

Thus with probability at least p , the maximum deviation from the expected mean is δ^* , which is why we simply assume this to be the case going forward, i.e.:

$$\frac{1}{n} \max_{i,j} \left(\left| (AHH_{role}^{(T)} - \mathbb{E}[AHH_{role}^{(T)}])_{i,j} \right| \right) < \frac{\delta}{3}$$

Consider the L1 distance of nodes inside the same cluster: This is at most $k\frac{\delta}{3}$. For nodes that belong to different clusters, this will be at least $k(\delta - 2\delta^*) > k\frac{\delta}{3}$. Therefore, the average linkage will combine all nodes belonging to the same role before it links nodes that belong to different roles. \square

Corollary E.1. Let $A^{(1)}, \dots, A^{(s)}$ be independent samples of the RIP model with the same role assignment (Ω_{role} must not necessarily be the same). Assuming the prerequisites of theorem 4.3 for $A = \frac{1}{s} \sum_{i=1}^s A^{(i)}$ - except eq. 8. If

$$s > -\frac{9\mathcal{W}_{-1}((q-1)\delta^2/9k^2)}{2n\delta^2}$$

Then with probability at least q : Algorithm 1 finds the correct role assignment using average linkage for clustering.